

UCLA

UCLA Previously Published Works

Title

Mapping genetic contributions to cardiac pathology induced by Beta-adrenergic stimulation in mice.

Permalink

<https://escholarship.org/uc/item/18c9s3dz>

Journal

Circulation. Cardiovascular genetics, 8(1)

ISSN

1942-325X

Authors

Rau, Christoph D
Wang, Jessica
Avetisyan, Rozeta
[et al.](#)

Publication Date

2015-02-01

DOI

10.1161/circgenetics.113.000732

Peer reviewed



Published in final edited form as:

Circ Cardiovasc Genet. 2015 February ; 8(1): 40–49. doi:10.1161/CIRCGENETICS.113.000732.

Mapping Genetic Contributions to Cardiac Pathology Induced by Beta-Adrenergic Stimulation in Mice

Christoph D. Rau, PhD^{1,*}, Jessica Wang, MD, PhD^{2,*}, Rozeta Avetisyan, BS¹, Milagros Romay, BS¹, Lisa Martin, PhD², Shuxun Ren, MD³, Yibin Wang, PhD³, and Aldons J. Lusis, PhD^{1,2}

¹Department of Microbiology, Immunology and Molecular Genetics, Department of Human Genetics, University of California, Los Angeles, CA

²Department of Medicine, Division of Cardiology, David Geffen School of Medicine, University of California, Los Angeles, CA

³Departments of Anesthesiology, Physiology and Medicine, Cardiovascular Research Laboratories, David Geffen School of Medicine, University of California, Los Angeles, CA

Abstract

Background—Chronic stress-induced cardiac pathology exhibits both a wide range in severity and a high degree of heterogeneity in clinical manifestation in human patients. This variability is contributed to by complex genetic and environmental etiologies within the human population. Genetic approaches to elucidate the genetics underlying the acquired forms of cardiomyopathies, including genome-wide association studies (GWAS), have been largely unsuccessful, resulting in limited knowledge as to the contribution of genetic variations for this important disease.

Methods and Results—Using the β -adrenergic agonist isoproterenol as a specific pathological stressor to circumvent the problem of etiological heterogeneity, we performed a GWAS for genes influencing cardiac hypertrophy and fibrosis in a large panel of inbred mice. Our analyses revealed 7 significant loci and 17 suggestive loci, containing an average of 14 genes, affecting cardiac hypertrophy, fibrosis and surrogate traits relevant to HF. Several loci contained candidate genes which are known to contribute to Mendelian cardiomyopathies in humans or have established roles in cardiac pathology based on molecular or genetic studies in mouse models. In particular, we identify *Abcc6* as the gene underlying a fibrosis locus by validating that an allele with a splice mutation of *Abcc6* dramatically and rapidly promotes isoproterenol induced cardiac fibrosis.

Conclusions—Genetic variants significantly contribute to the phenotypic heterogeneity of stress induced cardiomyopathy. Systems genetics is an effective approach to identify genes and pathways underlying the specific pathological features of cardiomyopathies. *Abcc6* is a previously unrecognized player in the development of stress-induced cardiac fibrosis.

Correspondence: Aldons J. Lusis, PhD, Department of Medicine/Division of Cardiology, A2-237 Center for the Health Sciences, UCLA School of Medicine, University of California, Los Angeles, CA 90095-1679, Tel: 310-825-1359, Fax: 310-794-7345, jlusis@mednet.ucla.edu; Yibin Wang, PhD, Department of Anesthesiology, Division of Molecular Medicine, University of California, Los Angeles, BH-569 CHS, Box 957115, Los Angeles, CA 90095-7115, Tel: 310-206-5197, Fax: 310-206-5907, yibinwang@mednet.ucla.edu.

*Contributed equally

Disclosures: The authors have declared that no competing interests exist.

Keywords

genomics; genome-wide association scan; catecholamine; mouse; heart failure

Introduction

Heart failure (HF) is a common cause of death with a lifetime risk of at least one in 9 for both men and women in developed countries¹. Heart failure is a complicated syndrome, characterized by a large number of pathological changes, such as contractile dysfunction, cardiomyocyte hypertrophy, edema and myocardial fibrosis²⁻⁴. The onset and severity of these pathological manifestations are highly heterogeneous among HF patients, likely due to complex interactions between the genetic variants and the pathological stressors including mechanical overload and humoral overstimulation. Indeed, a number of humoral factors such catecholamines and angiotensin II are known to play key roles in triggering HF; however, the genetic variations underlying the pathological outcome in response to these stressors remains elusive. Dissecting the genetic contributions to specific pathological changes in the failing heart would provide important insights for the future development of personalized diagnoses and targeted therapies.

In contrast to many other common disorders, GWAS of HF have had modest success in elucidating the genetics underlying this complex disease. Only two heart-failure related loci⁵ have reached accepted levels of genome-wide significance, despite meta-analyses of tens of thousands of patients^{6,7}. The challenge of performing GWAS in human HF is likely due to the very complex nature of the disease, which can arise as a result of multiple underlying etiologies, such as myocardial infarction, hypertension or metabolic disorders, each of which are complex traits with significant environmental confounders¹. Attempts to dissect the genetics of HF traits in rodents have been only modestly successful; although a number of loci for hypertrophy and fibrosis have been identified, the poor mapping resolution of traditional linkage analyses has complicated the identification of the underlying genes⁸⁻¹¹. The development of a method to perform high resolution, association-based mapping of complex traits in mice¹² provided an opportunity to identify genetic factors contributing to common forms of HF under defined stress conditions.

In this study, we have conducted a comprehensive phenotypic characterization in a large panel of densely genotyped inbred mice from the Hybrid Mouse Diversity Panel (HMDP)¹² following chronic treatment with a β -adrenergic agonist, isoproterenol (ISO). A wide spectrum of phenotypic changes was observed among the HMDP mice in ISO induced cardiac hypertrophy, fibrosis and peripheral edema. Using GWAS, we uncovered 7 significant loci and 17 suggestive loci, each containing an average of 14 genes. Several of these loci included genes with established causal roles in familial cardiomyopathies in humans or heart failure phenotypes in experimental models. In addition, we identified *Abcc6* as a previously unrecognized regulator of ISO-induced cardiac fibrosis. Therefore, our study demonstrates clear evidence that genetic variants have a significant contribution to the phenotypic heterogeneity of stress-induced cardiomyopathy.

Materials and Methods

Ethics Statement

All animal experiments were conducted following guidelines established and approved by the University of California, Los Angeles Institutional Animal Care and Use Committee. All surgery and echocardiography was performed under isoflurane anesthesia, and every effort was made to minimize suffering.

Online database

All results and data can be accessed at <http://systems.genetics.ucla.edu/data>

Mice and isoproterenol treatment

The mouse strains listed in Table S1 were obtained from The Jackson Laboratory and then bred in our colony. All mice have been previously genotyped at over 130,000 locations. Isoproterenol (30 mg per kg body weight per day, Sigma) was administered for 21 d in 8- to 10-week-old female mice using ALZET osmotic minipumps, which were surgically implanted intra-peritoneally.

Abcc6 KO and transgenic mice^{13,14} underwent the same protocol as described above, although both male and female mice were used in the analysis. No significant difference between genders was observed as a result of ISO treatment in these KO and transgenic animals.

Heart Weights

At day 21, mice were sacrificed and body weight recorded. The heart was removed and weighed, then separated into its four component chambers, each of which was individually weighed as well. Each chamber of the heart was immediately frozen in liquid nitrogen for any future analysis and stored in a -80° freezer. Lung and liver were removed and weighed. Additionally, the adrenal glands were removed, weighed and frozen in liquid nitrogen.

Fibrosis and Calcification

A portion of the left ventricle was placed in formalin for at least 48 hrs for preservation of ultrastructure. These samples were then washed with distilled water and sent to UCLA Department of Pathology and Laboratory Medicine for paraffin embedding and staining using Masson's Trichrome for fibrosis and Alizarin Red for calcification. Sections were analyzed using a Nikon Eclipse, TE2000-U microscope and images captured of the entire cross-section of the heart. Fibrosis was quantified using the Nikon Imagine System Elements AR program by comparing the amount of tissue stained blue (for collagen) or red (for calcification) to the total tissue area. To confirm our results, we examined a subset of the strains using Sirius Red, another fibrosis-marking stain, and observed high concordance between our samples ($R=0.75$, data not shown). As expected^{4,15}, we observed strong correlations between cardiac fibrosis and total heart weight ($P=1.1E-07$). Our results compare favorably to prior quantifications of fibrosis in a limited number of strains¹⁶.

Mice used for the *Abcc6* validation experiments underwent an identical protocol to the one described above for Masson Trichrome and Alizarin Red staining, using five sections per heart for both Trichrome and Alizarin Red staining.

Echocardiography

Transthoracic echocardiograms were performed using the Vevo 770 ultrasound system (VisualSonics, Inc., Toronto, ON, Canada). Inhaled isoflurane (1.25% during induction and 1% during maintenance) was administered to ensure adequate sedation while maintaining heart rate above 450 beats per minute. A parasternal long-axis B-mode image was obtained. The maximal long-axis of the left ventricle (LV) was positioned perpendicular to the ultrasound beam. A 90° rotation of the ultrasound probe at the papillary muscle level was performed to obtain a parasternal short-axis view of the LV. A M-mode image was captured to document LV dimensions. Then a semi-apical long-axis view of the LV was obtained. The LV ejection time, E and A wave velocities were obtained from this view using pulse wave Doppler. Images were saved for analysis at a later time point using the Vevo 770 cardiac analysis package. In summary, a baseline echocardiogram was performed on all of the mice. Among control mice, a second echocardiogram was performed in 70 mouse strains at week 3. In isoproterenol-treated mice, serial echocardiograms were performed at 1, 2, and 3 weeks. A single operator, who followed a standard operating protocol detailed above, performed all of the echocardiograms. Saved images were analyzed at a later time point by a single observer who was blinded to mouse strains.

Association Analysis

Unless otherwise noted, all analyses were performed using the R software environment. We performed the association testing of each SNP with a linear mixed model, which accounts for the population structure among the n animals using the following model¹⁷:

$$y = 1_n + m + xb + u + e$$

where m is the mean, b is the allele effect of the SNP, x is the $(n \times 1)$ vector of observed genotypes of the SNP (using additive coding of 0,0.5,1), u is the random effects due to genetic relatedness with $var(u) = \sigma_u^2 K$, and e is the random noise with $var(e) = \sigma_e^2 I$. K denotes the identity-by-state kinship matrix estimated from all the SNPs, I denotes the $(n \times n)$ identity matrix, and 1_n is the $(n \times 1)$ vector of ones. We estimated σ_u^2 and σ_e^2 using restricted maximum likelihood (REML) and computed p values using the standard F test to test the null hypothesis $b=0$. All phenotypes were examined for deviation from normality by visual examination of a normal probability plot. The right ventricular ratio phenotype was found to deviate somewhat from normality, however in order to keep the analysis consistent across phenotypes, no transformation of the data was performed. Prior work¹⁷ has demonstrated that for the HMDP, $4.1E-6$ is the correct significance threshold for a single trait. We conservatively estimated that we were observing ten independent phenotypes in our data and determined our final significance threshold, $4.1E-7$, by Bonferroni correction. LD was determined by calculated pairwise SNP correlations for each chromosome. Approximate LD boundaries were determined by visualizing > 0.8 correlations in MATLAB (MathWorks).

Locus Overlap with Other Studies

Gwas.gov was queried for all human GWAS loci for the terms ‘heart failure’ or ‘cardiac hypertrophy.’ All loci with p -value $< 5E-7$ were selected. The NCBI homology maps (<http://www.ncbi.nlm.nih.gov/projects/homology/maps/>) were used to find syntenic location of the 5 Mb region surrounding the peak SNP of the human HF locus. If a mapped syntenic region overlapped with the LD block of a suggestive locus from our study, it was considered a positive hit. A significance p -value was obtained by permutation testing, in which all suggestive loci were randomly placed across the genome and the number of overlaps measured a total of 100,000 times. Final significance was calculated as the number of permutations which surpassed the observed number of overlaps.

Microarray and eQTL analysis

Following homogenization of left ventricular tissue samples in QIAzol, RNA was extracted using the Qiagen miRNAeasy extraction kit, and verified as having a RIN > 7 by Agilent Bioanalyzer. Two RNA samples were pooled for each strain/experimental condition, whenever possible, and arrayed on Illumina Mouse Reference 8 version 2.0 chips. Analysis was conducted using the Neqc algorithm included in the limma R package¹⁸ and batch effects addressed through the use of COMBAT¹⁹. eQTLs were then calculated for 13,155 expressed genes using EMMA, as described above. Significance thresholds were calculated as in Parks et al.²⁰ Briefly, *cis*-eQTLs were calculated using a FDR of 5% for all SNPs that lay within 1 Mb of any probe (roughly 100 SNPs), using standard permutation analysis methods (total of 100 permutations of all data), previously used for *cis*-eQTL analysis.^{21–23} Our determined cutoff of $3.6E-3$ further takes into account linkage disequilibrium which further reduces the effective number of SNPs in each 2 Mb window surrounding the peak SNP. We have previously observed that *cis*-eQTL at this level are highly conserved in the HMDP.²⁴ *Trans*-eQTLs were calculated using the overall HMDP cutoff as determined in Kang et al. and described above.¹⁷

Results

Pathological Analysis of ISO Induced Cardiomyopathy in HMDP Mice

β -adrenergic stimulation is considered a common and critical driving force behind ongoing hypertrophy and progression to heart failure²⁵. We treated mice chronically with isoproterenol (ISO), a synthetic non-selective β -adrenergic agonist^{26,27}. 748 mice from 105 different strains of the Hybrid Mouse Diversity Panel (HMDP) were divided into control (average 2.2 per strain) and treated (average 4.1 per strain) cohorts (Table S1). Treated mice were implanted with an Alzet micropump and given 30 mg/kg/day of ISO for three weeks, at which point all mice were sacrificed. We characterized a variety of phenotypes to capture specific portions of the complex heart failure syndrome. For this report, cardiac hypertrophy and pulmonary and liver edema were assessed by measuring the weights of the four cardiac chambers, the lungs and the liver. Cardiac fibrosis, a phenotype which is very difficult to study in humans, was measured by histological quantification of fibrotic tissue area as a percentage of all tissue area in left ventricular sections stained using Masson Trichrome. Functional analysis of the mouse hearts were performed using echocardiography. We observed statistically significant correlations between our calculated left ventricular weights

from echocardiography and our measured left ventricular weights after harvesting ($R=0.82$, $P=5E-24$) as well as between left ventricular weight and left ventricular internal dimension ($R=0.26$, $P=1.3E-11$). Further analysis of the functional data, including association analyses for each observed functional phenotype are still under preparation and will be reported in a subsequent manuscript.

As shown in Fig. 1, we observed striking differences in cardiac hypertrophy, fibrosis, and degrees of pulmonary and hepatic edema among the strains. Our results are consistent with another report from a more limited strain survey²⁸. After treatment with ISO, mice were slightly heavier than their paired controls (23.5 g vs. 21.83 g, $p=0.009$), likely due to edema. We observed a far more significant increase in weight for our traits of interest such as total heart weight ($P=5.3E-24$) and lung weight ($4.6E-12$) (Table S2). Although it is likely that the ISO-treated organ weights are influenced by the slight increase in body weight, the magnitude of the results we observe in our study leads us to conclude that this influence is minimal when compared to the direct effects of ISO stimulation on the heart itself.

Of the 470 mice assigned to the treatment cohort, 139 (29.6%) died prior to the end of the protocol, most (127) within the first 48 hours of treatment, whereas none of the control cohort died (Fig. S1). There was no observable significant differences in baseline conditions between mice which survived the initial ISO challenge and mice which died after ISO challenge. Furthermore, we did not observe significant correlation between the strains which showed high mortality prior to end of protocol and any of our expressed genes before or after treatment (the most significant correlation was for the Riken gene 8430432M10RIK ($R^2=0.16$, $P=5.6E-5$), which fails to satisfy a Bonferroni-corrected threshold of $3E-6$). Among the phenotypic traits (Bonferroni threshold $4.8E-4$), we observed that the post-ISO Mean Normalized Systolic Ejection Rate functional trait demonstrated significant correlation ($R^2=0.14$, $P=3E-4$) with premature mortality. This relationship will be explored in greater detail in our manuscript focusing on echocardiographic functional traits. GWA on this premature death trait revealed a single locus (peak SNP rs29166005, $P=9E-6$) which contributes suggestively to this phenotype. These results suggest that the cause of our observed ISO-induced death is likely linked to underlying genetic effects and/or the interaction between genes and the ISO treatment.

Genomewide Association

Association analysis was performed using ~132,000 SNPs across the genome with the EMMA algorithm¹⁷ to correct for population structure. In addition to the absolute tissue weight measurements, analyses were performed on the ratios of each treated weight to its corresponding control weight as a measure of responsiveness to ISO treatment. Prior work with EMMA and the HMDP, employing simulation and permutation, has suggested that an appropriate genome-wide significance threshold for a single trait is $4.1E-06$ ¹². This is approximately equivalent to a Bonferroni correction¹². To correct for multiple comparisons, we have chosen the threshold of $4.1E-07$ and a minimum minor allele frequency (MAF) of 7.5% for our study. Given that the traits are correlated, this threshold (10-fold lower than the genome-wide significance level for a single trait) is conservative. Using these thresholds, we have identified 7 significant loci and 17 additional loci which matched the nominal

significance threshold of $4.1E-06$ (Tables 1, 2, S3). While linkage analysis in mice typically exhibits a resolution of tens of Mb^{8,29}, the loci identified in this study averaged 1–2 Mb in size, based on linkage disequilibrium, with the majority being less than 1 Mb.

The right and left ventricular weight (RVW, LVW) variations mirrored each other closely, with associations being somewhat stronger for RVW (Fig. 1b), although each locus identified in the right ventricle was also detected at a lower level of significance in the left ventricle (Fig. S2). In total we observed three significant and five suggestive loci corresponding to treated RVW (Fig. 2a), one significant and one suggestive locus for the ratio of treated to untreated RVW (Fig. 2b) and a single suggestive locus for the ratio of right atrial weight. Similar to the heart weights, we observed marked variation of liver and lung weights following ISO treatment across the HMDP (Fig. 1c, 1d). Lung weight in particular showed a robust increase with ISO treatment. We observed one significant and four suggestive loci corresponding to ISO-treated lung weights (Fig. 2c), and one significant and one suggestive locus corresponding to ISO-treated liver weights (Fig. 2d). Cardiac fibrosis also varied significantly in both baseline and treated mice, with the extent of fibrosis being much greater in treated mice (Fig. 1e). We observed a total of three suggestive loci for cardiac fibrosis in untreated animals (Fig. 2e), and one significant and four suggestive loci in treated animals (Fig. 2f).

eQTL Analysis for Candidate Genes from ISO treated HMDP Mice

To help identify candidate genes at the heart failure associated loci, we carried out global expression analysis of left ventricular heart tissue from 92 strains of ISO treated mice. The loci controlling gene expression levels were mapped using EMMA, and are referred to as expression quantitative trait loci (eQTL). eQTLs were termed ‘*cis*’ if the locus maps within 1Mb of the gene and otherwise were termed ‘*trans*’. Overall, we observed 3093 *cis* eQTL (FDR 5%= $P < 3.6E-3$, in line with previous measures in the HMDP²⁰). Additionally, the Wellcome Trust Mouse Genomes Project sequencing database³⁰, which has the full genomic sequence of 10 strains in our panel, was utilized to examine genomic variations, such as missense, nonsense or splicing variations, in each locus. Together, these two approaches provided a powerful and systematic method for the identification of causal genes within each locus. All significant and suggestive loci as well as gene expression data are available at <http://systems.genetics.ucla.edu/data>.

Using eQTL analysis combined with GWAS, we identified a causal gene in one of the cardiac hypertrophy loci on chromosome 3 (Fig. 3). The peak SNP ($P=1.9E-6$), for the trait of treated-to-untreated right RVW ratio, lies between the second and third exons of *Ppp3ca*, encoding the alpha isozyme of calcineurin A, which is also the only gene contained within the Linkage Disequilibrium (LD) block surrounding the significantly associated SNPs. Calcineurin A is a known target of β -adrenergic signaling, with a well-described role in ISO-induced hypertrophy²⁶. Calcineurin A is the only gene in LD with the peak SNP and has a significant *cis*-eQTLs ($P=1.3E-3$) for the ratio of treated to control calcineurin A expression (Fig. 3a,b). We also observed a modest correlation between the ratio of *Ppp3ca* expression and the ratio of heart weights in control and ISO-treated animals ($R=-0.18, P=0.01$). We further observed *Ppp3cb*, the beta isozyme of calcineurin A, in a locus on chromosome 14

($P=3.3E-6$) for the trait treated lung weight. *Ppp3cb* has a strongly suggestive *cis*-eQTL ($P=4.7E-3$) as well as a minor allele with an insertion in a splice site in several strains of the HMDP. In addition to calcineurin A, we identified several other genes with well-established roles in cardiac physiology and pathology within other disease-associated loci. These include the key calcium cycling regulator phospholamban³¹ and structural protein *Sgcd*³² as well as other genes which have previously been implicated in cardiac hypertrophy such as *Prkag2*³³, or cardiac malformation, such as *Mospd3*³⁴ (Tables 1 and 2).

The Database for Annotation, Visualization and Integrated Discovery (DAVID)^{35,36} was used to examine the genes located within linkage disequilibrium of the peak SNPs of our study. We observed significant enrichment for calmodulin-related genes (benjamini-corrected $P=0.02$) and suggestive enrichment categories such as calcium signaling (uncorrected $P=0.003$) and EGF signaling ($p=0.009$), both of which lie downstream of β -adrenergic signaling (Table S6). Examination of our top candidate genes within each locus reveals a strong bias towards genes known to be involved in catecholamine-stimulated cardiomyopathy such as calcineurin, phospholamban and calmodulin (Tables 1 and 2)

Conservation of Cardiomyopathy Loci in Mice and Humans

We explored whether the loci we identified overlap with human GWAS results by examining the top twelve previously identified significant and suggestive human loci^{6,7,37}. The human loci were mapped onto the mouse genome using the NCBI Homologene resource and compared to a set of loci identified for the weight traits based on a slightly relaxed stringency ($P<1E-05$, $MAF>5\%$) from the HMDP study. We observed six out of twelve human loci, including one of the genome-wide significant loci near *USP3*, replicating in our study (Table S4). We determined that this overlap is highly significant ($P=3.5E-4$) by permutation analysis. Our result supports the concept that genetic influences in β -adrenergic signaling significantly contribute to polygenic human HF. Furthermore, sixteen loci for HF-related traits have previously been identified via linkage studies in mice for HF-related traits. We further observed that seven of these sixteen QTLs overlap with weight loci identified in this study ($P=1.2E-3$ by permutation analysis) (Table S5), despite the fact that some of the linkage studies utilized different hypertrophy-inducing stressors such as a calsequestrin transgene⁸, which likely influence distinct HF pathways.

Validation of *Abcc6* as Causal Gene for ISO Induced Cardiac Fibrosis

We have identified a locus contributing to ISO-induced fibrosis on chromosome 7 (Fig. 4, $P=7.1E-7$). One of the 28 genes within the LD block, *Abcc6*, has a splice site variation³⁸ resulting in a premature stop codon that is found in 19 of the strains we analyzed for cardiac fibrosis (KK/HiJ, C3H/HeJ, DBA/2J, 11 BxD, 2 BxH, 3 CxB) in the HMDP. In untreated animals, we did not observe any significant difference ($P=0.25$) between the degrees of fibrosis present in the left ventricle among HMDP strains divided based on *Abcc6* genotype. In contrast, we observed a marked increase in cardiac fibrosis in the mice containing the *Abcc6* splice mutation allele in response to ISO treatment ($P=1E-4$) (Fig. 4B). *Abcc6* deficiency is the cause of pseudoxanthoma elasticum, a disorder characterized by progressive tissue calcification^{13,39}, and a deficiency of *Abcc6* has previously been linked to calcification phenotypes in aged mice by our laboratory³⁸. However, the fibrosis phenotype

observed in these studies is clearly distinct from that of calcification. In fact, we did not observe a significant association with heart calcification in our study under basal ($P=0.8$) or ISO treatment condition ($P=0.12$) in mice with different *Abcc6* genotypes, although we did observe some outlier strains such as KK/HIJ, that had markedly increased calcification after ISO stimulation (Fig. 4C). Therefore, *Abcc6* is a likely candidate gene contributing to ISO induced fibrosis in heart.

To validate the role of *Abcc6* in cardiac fibrosis, we studied a previously described *Abcc6* knockout mouse carrying a targeted mutation in a C57BL/6J strain background (KO) as well as the wildtype C57BL/6J (Control) mice¹³. We previously reported that the *Abcc6* KO mice exhibited increased cardiac calcification beginning from 6 months of age¹⁴. At three months of age, neither the wild type nor the KO mice exhibited significant differences in calcification as judged by Alizarin Red staining or cardiac fibrosis based on Masson Trichrome staining in the absence of ISO treatment (Fig. 4D). Consistent with our observations of the entire panel, the ISO treatment significantly increased fibrosis levels in the *Abcc6* KO animals without significantly increasing calcification levels in these mice. This result suggests that the age-associated calcification phenotype observed in *Abcc6* KO is distinct from the ISO-induced cardiac fibrosis phenotype.

To further establish *Abcc6* as a causal gene for ISO induced cardiac fibrosis, we studied transgenic mice carrying the *Abcc6* wildtype locus from a C57BL/6J bacterial artificial chromosome (BAC) on the background of the fibrosis-susceptible C3H/HeJ strain. Strain C3H/HeJ mice lack functional *Abcc6* due to a splice variation⁴⁰. In the absence of ISO neither C3H/HeJ mice nor C3H/HeJ mice carrying the *Abcc6* BAC-transgene exhibited significant calcification or fibrosis in the heart, whereas after ISO treatment the C3H/HeJ mice but not the *Abcc6*-BAC transgenic mice exhibited substantial fibrosis and calcification (Fig. 4E). The differing results between the C57BL/6J KO mice and the naturally mutant C3H/HeJ mice suggests that additional modifier genes are necessary to induce cardiac calcification in *Abcc6* KO mice after ISO stimulation, whereas *Abcc6* KO is sufficient to cause ISO-induced cardiac fibrosis. The mechanisms by which *Abcc6* promotes fibrosis is unknown, but DAVID analysis of genes significantly correlated with *Abcc6* expression in heart showed highly significant enrichment for mitochondrial genes (Table S7). Systemic factors are clearly involved in the calcification phenotype of *Abcc6* deficiency⁴⁰, but it is noteworthy that, based on our expression profiling data, *Abcc6* is clearly expressed in heart. The *Abcc6* locus is suggestively associated ($P<0.01$) with several hypertrophic phenotypes in our study, namely whole heart weight ($P=4E-3$), right atrial weight ($P=5E-3$) and left ventricle weight ($P=7E-3$). Transcript co-expression network analysis was performed on *Abcc6*, but the module into which *Abcc6* fell was not significantly enriched for any particular GO term using DAVID (data not shown).

Discussion

We have used a strategy involving GWAS in a large panel of inbred mice to perform fine mapping of loci contributing to specific pathological features of cardiomyopathy following treatment with ISO^{26,27}. We have combined this strategy with global gene expression analysis in the heart to help identify candidate genes. A significant number of genetic loci

revealed from this study are replicated in human GWAS analysis, supporting a conserved genetic network contributing to human heart failure. A number of the loci contain genes known to be involved in cardiomyopathy based on previous biochemical or genetic studies, supporting the validity of this approach to uncover important mechanisms and pathways related to the onset of heart failure. Finally, we validated *Abcc6* a candidate GWAS hit, as a novel player in stress-induced cardiac fibrosis. These findings should complement human studies to identify genes and pathways contributing to this very common and poorly understood disorder.

Systems genetics is a potent approach to reveal genes and pathways underlying the specific pathological features of cardiomyopathies, of which GWAS represents only one potential avenue for exploration. Using the resources presented here, it should be possible to perform additional analyses, including the generation of transcript co-expression networks for the identification of groups of genes involved in maladaptive cardiac remodeling. The genetic information and the phenotypic spectra established by this study should provide a valuable resource for future heart failure studies.

Supplementary Material

Refer to Web version on PubMed Central for supplementary material.

Acknowledgments

The authors wish to thank the excellent technical assistance from Ms. Mary Tuteryan, Ms. Haiying Pu and Ms. Melenie Rosales.

Funding Sources: This work was supported by NIH grants HL110667 and HL28481. CDR was supported by NIH training grant T32HL69766 and JW was supported by NIH training grant HL007895.

References

1. Mudd JO, Kass DA. Tackling heart failure in the twenty-first century. *Nature*. 2008; 451:919–928. [PubMed: 18288181]
2. Beltrami CA, Finato N, Rocco M, Feruglio GA, Puricelli C, Cigola E, et al. Structural basis of end-stage failure in ischemic cardiomyopathy in humans. *Circulation*. 1994; 89:151–163. [PubMed: 8281642]
3. Frangiannis NG. Regulation of the inflammatory response in cardiac repair. *Circ Res*. 2012; 110:159–173. [PubMed: 22223212]
4. Kong P, Christia P, Frangiannis NG. The pathogenesis of cardiac fibrosis. *Cell Mol Life Sci*. 2014; 71:549–574. [PubMed: 23649149]
5. Villard E, Perret C, Gary F, Proust C, Dilanian G, Hengstenberg C, et al. A genome-wide association study identifies two loci associated with heart failure due to dilated cardiomyopathy. *Eur Heart J*. 2011; 32:1065–1076. [PubMed: 21459883]
6. Morrison AC, Felix JF, Cupples LA, Glazer NL, Loehr LR, Dehghan A, et al. Genomic variation associated with mortality among adults of European and African ancestry with heart failure: the cohorts for heart and aging research in genomic epidemiology consortium. *Circ Cardiovasc Genet*. 2010; 3:248–255. [PubMed: 20400778]
7. Parsa A, Chang Y-PC, Kelly RJ, Corretti MC, Ryan Ka, Robinson SW. Hypertrophy-associated polymorphisms ascertained in a founder cohort applied to heart failure risk and mortality. *Clin Transl Sci*. 2011; 4:17–23. [PubMed: 21348951]

8. Le Corvoisier P, Park H-Y, Carlson KM, Marchuk DA, Rockman HA. Multiple quantitative trait loci modify the heart failure phenotype in murine cardiomyopathy. *Hum Mol Genet.* 2003; 12:3097–3107. [PubMed: 14519689]
9. McDermott-Roe C, Ye J, Ahmed R, Sun X-M, Serafín A, Ware J, et al. Endonuclease G is a novel determinant of cardiac hypertrophy and mitochondrial function. *Nature.* 2011; 478:114–118. [PubMed: 21979051]
10. Wheeler FC, Fernandez L, Carlson KM, Wolf MJ, Rockman Ha, Marchuk DA. QTL mapping in a mouse model of cardiomyopathy reveals an ancestral modifier allele affecting heart function and survival. *Mamm Genome.* 2005; 16:414–423. [PubMed: 16075368]
11. Wheeler FC, Tang H, Marks OA, Hadnott TN, Chu P-L, Mao L, et al. Tnni3k modifies disease progression in murine models of cardiomyopathy. *PLoS Genet.* 2009; 5:e1000647. [PubMed: 19763165]
12. Bennett BJ, Farber CR, Orozco L, Kang HM, Ghazalpour A, Siemers N, et al. A high-resolution association mapping panel for the dissection of complex traits in mice. *Genome Res.* 2010; 20:281–290. [PubMed: 20054062]
13. Mungrue IN, Zhao P, Yao Y, Meng H, Rau C, Havel JV, et al. Abcc6 deficiency causes increased infarct size and apoptosis in a mouse cardiac ischemia-reperfusion model. *Arterioscler Thromb Vasc Biol.* 2011; 31:2806–2812. [PubMed: 21979437]
14. Martin LJ, Lau E, Singh H, Vergnes L, Tarling EJ, Mehrabian M, et al. ABCC6 localizes to the mitochondria-associated membrane. *Circ Res.* 2012; 111:516–520. [PubMed: 22811557]
15. Berk BC, Fujiwara K, Lehoux S. Review series ECM remodeling in hypertensive heart disease. 2007; 117:568–575.
16. Bronson, RT. Rate of occurrence of lesions in 20 inbred and hybrid genotypes of rats and mice sacrificed at 6-month intervals during the first years of life. In: Harrison, D., editor. *Genetic Effects of Aging II.* Caldwell, NJ: Telford Press; 1990. p. 279-358.
17. Kang HM, Zaitlen NA, Wade CM, Kirby A, Heckerman D, Daly MJ, et al. Efficient control of population structure in model organism association mapping. *Genetics.* 2008; 178:1709–1723. [PubMed: 18385116]
18. Smyth, GK. No Title. In: Gentleman, R.; Irizarry, W.; Huber, W., editors. *Bioinformatics and Computational Biology Solutions using R and Bioconductor.* New York: Springer; 2005. p. 397-420.
19. Johnson WE, Li C, Rabinovic A. Adjusting batch effects in microarray expression data using empirical Bayes methods. *Biostatistics.* 2007; 8:118–127. [PubMed: 16632515]
20. Parks BW, Nam E, Org E, Kostem E, Norheim F, Hui ST, et al. Genetic control of obesity and gut microbiota composition in response to high-fat, high-sucrose diet in mice. *Cell Metab.* 2013; 17:141–152. [PubMed: 23312289]
21. Grundberg E, Small KS, Hedman ÅK, Nica AC, Buil A, Keildson S, et al. Mapping cis- and trans-regulatory effects across multiple tissues in twins. *Nat Genet.* 2012; 44:1084–1089. [PubMed: 22941192]
22. Borel C, Deutsch S, Letourneau A, Migliavacca E, Montgomery SB, Dimas AS, et al. Identification of cis- and trans-regulatory variation modulating microRNA expression levels in human fibroblasts. *Genome Res.* 2011; 21:68–73. [PubMed: 21147911]
23. Nica AC, Ongen H, Irminger J-C, Bosco D, Berney T, Antonarakis SE, et al. Cell-type, allelic, and genetic signatures in the human pancreatic beta cell transcriptome. *Genome Res.* 2013; 23:1554–1562. [PubMed: 23716500]
24. Hasin-Brumshtein Y, Hormozdiari F, Martin L, van Nas A, Eskin E, Lusk AJ, et al. Allele specific expression and eQTL analysis in mouse adipose tissue. *BMC Genomics.* 2014; 15:471. [PubMed: 24927774]
25. Dorn GW, Liggett SB. Pharmacogenomics of beta-adrenergic receptors and their accessory signaling proteins in heart failure. *Clin Transl Sci.* 2008; 1:255–262. [PubMed: 20443857]
26. Breckenridge R. Heart failure and mouse models. *Dis Model Mech.* 2010; 3:138–143. [PubMed: 20212081]
27. Zhang X, Szeto C, Gao E, Tang M, Jin J, Fu Q, et al. Cardiotoxic and Cardioprotective Features of Chronic β -Adrenergic Signaling. *Circ Res.* 2013; 112:498–509. [PubMed: 23104882]

28. Berthonneche C, Peter B, Schüpfer F, Hayoz P, Kutalik Z, Abriel H, et al. Cardiovascular response to beta-adrenergic blockade or activation in 23 inbred mouse strains. *PLoS One*. 2009; 4:e6610. [PubMed: 19672458]
29. Flint J, Eskin E. Genome-wide association studies in mice. *Nat Rev Genet*. 2012; 13:807–817. [PubMed: 23044826]
30. Yalcin B, Wong K, Agam A, Goodson M, Keane TM, Gan X, et al. Sequence-based characterization of structural variation in the mouse genome. *Nature*. 2011; 477:326–329. [PubMed: 21921916]
31. Schönberger J, Seidman CE. Many roads lead to a broken heart: the genetics of dilated cardiomyopathy. *Am J Hum Genet*. 2001; 69:249–260. [PubMed: 11443548]
32. Bauer R, Macgowan GA, Blain A, Bushby K, Straub V. Steroid treatment causes deterioration of myocardial function in the {delta}-sarcoglycan-deficient mouse model for dilated cardiomyopathy. *Cardiovasc Res*. 2008; 79:652–661. [PubMed: 18495669]
33. Banerjee SK, McGaffin KR, Huang XN, Ahmad F. Activation of cardiac hypertrophic signaling pathways in a transgenic mouse with the human PRKAG2 Thr400Asn mutation. *Biochim Biophys Acta*. 2010; 1802:284–291. [PubMed: 20005292]
34. Pall GS, Wallis J, Axton R, Brownstein DG, Gautier P, Buerger K, et al. A novel transmembrane MSP-containing protein that plays a role in right ventricle development. *Genomics*. 2004; 84:1051–1059. [PubMed: 15533722]
35. Dennis G, Sherman BT, Hosack DA, Yang J, Gao W, Lane HC, et al. DAVID: Database for Annotation, Visualization, and Integrated Discovery. *Genome Biol*. 2003; 4:P3. [PubMed: 12734009]
36. Huang DW, Sherman BT, Lempicki RA. Systematic and integrative analysis of large gene lists using DAVID bioinformatics resources. *Nat Protoc*. 2009; 4:44–57. [PubMed: 19131956]
37. Ellinor PT, Sasse-Klaassen S, Probst S, Gerull B, Shin JT, Toepfel A, et al. A novel locus for dilated cardiomyopathy, diffuse myocardial fibrosis, and sudden death on chromosome 10q25–26. *J Am Coll Cardiol*. 2006; 48:106–111. [PubMed: 16814656]
38. Meng H, Vera I, Che N, Wang X, Wang SS, Ingram-Drake L, et al. Identification of Abcc6 as the major causal gene for dystrophic cardiac calcification in mice through integrative genomics. *Proc Natl Acad Sci U S A*. 2007; 104:4530–4535. [PubMed: 17360558]
39. Campens L, Vanakker OM, Trachet B, Segers P, Leroy BP, De Zaeytjijd J, et al. Characterization of Cardiovascular Involvement in Pseudoxanthoma Elasticum Families. *Arterioscler Thromb Vasc Biol*. 2013; 33:2646–2652. [PubMed: 23968982]
40. Jiang Q, Oldenburg R, Otsuru S, Grand-Pierre AE, Horwitz EM, Uitto J. Parabiogenic heterogenetic pairing of Abcc6^{-/-}/Rag1^{-/-} mice and their wild-type counterparts halts ectopic mineralization in a murine model of pseudoxanthoma elasticum. *Am J Pathol*. 2010; 176:1855–1862. [PubMed: 20185580]

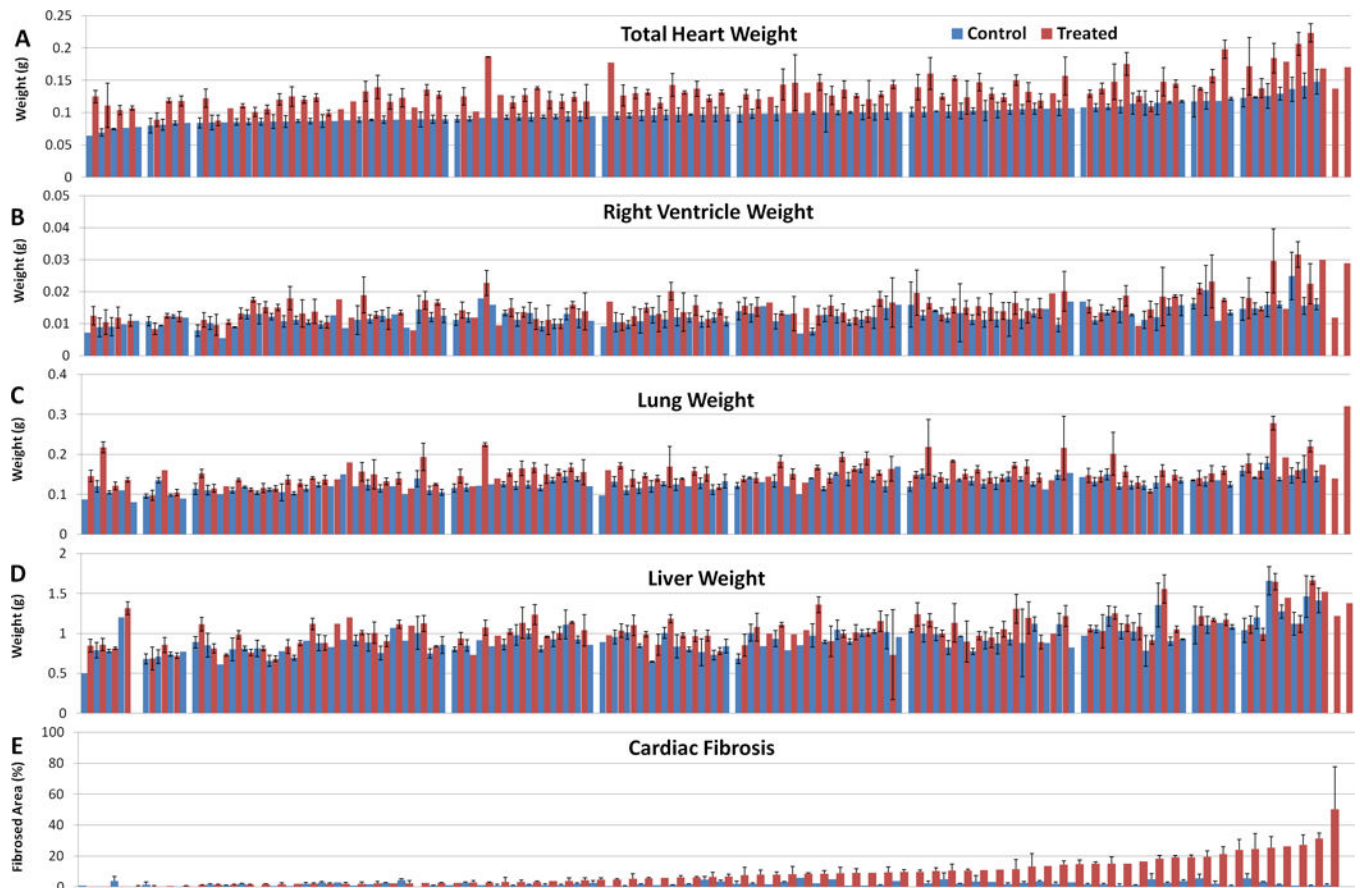


Figure 1. Wide variation in HF traits between the strains of the HMDP. **A)** Total Heart Weight **B)** Right Ventricular Weight **C)** Lung Weight **D)** Liver Weight. **E)** Cardiac Fibrosis. A–D are organized by the untreated heart weight of the strain and display mean \pm standard deviation. For enlarged figures with strain names, see figures S3–S7

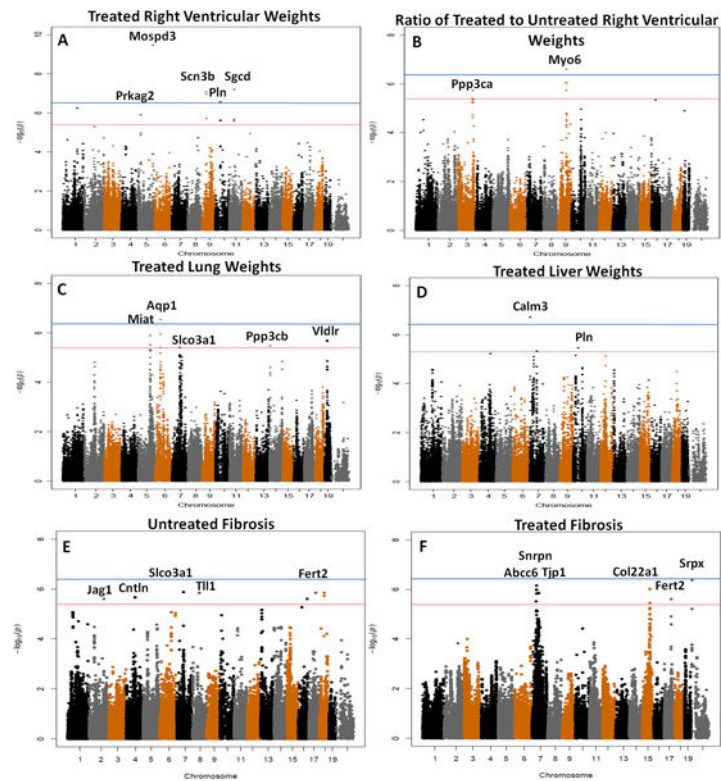


Figure 2. Manhattan plots of HF traits **A)** treated right ventricular weights **B)** ratio of treated to untreated right ventricular weights **C)** treated lung weights **D)** treated liver weights. **E)** baseline cardiac fibrosis and **F)** treated cardiac fibrosis. The red line indicates the threshold for suggestive association ($4.2E-6$) between a SNP and a phenotype while the blue line indicates the threshold for significant association ($4.2E-7$). Proposed candidate genes are indicated by gene symbols above peaks. QQ plots for each phenotype may be found in supplemental figure S8

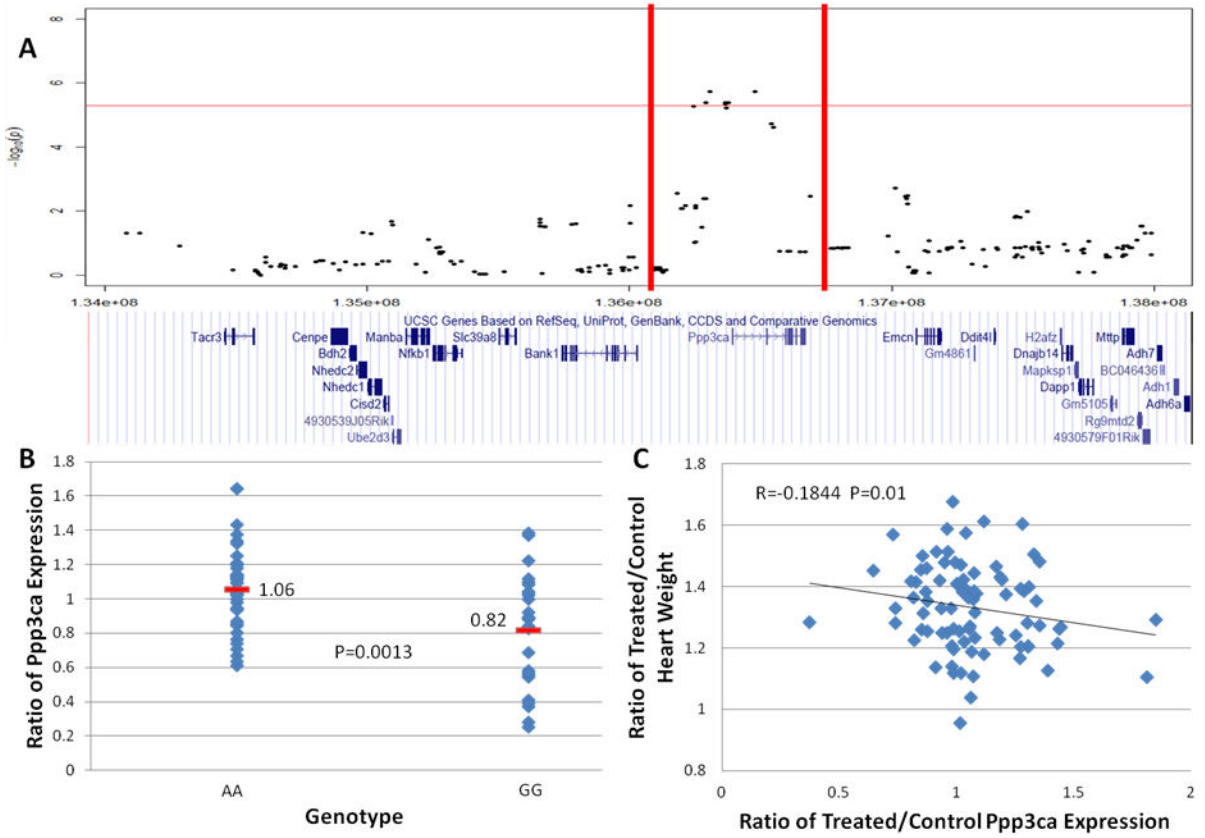


Figure 3. *Ppp3ca* (calcineurin A) is a candidate gene at the Chromosome 3 right ventricular weight ratio locus. **A)** *Ppp3ca* is the only gene within the locus. The red horizontal line represents the significance threshold, while the red vertical lines indicate the limits of the Linkage disequilibrium block. The dots represent SNPs, plotted in basepairs along the chromosome with $-\log_{10}(p)$ value on the Y axis. Below are the locations of genes from a genome browser. **B)** *Ppp3ca* has a significant *cis*-eQTL ($P=1.3E-3$) for the ratio of gene expression after and before treatment. Red line and number indicate average gene expression **C)** The ratio of *Ppp3ca* expression has significant ($P=0.01$) negative correlation with the ratio of treated to untreated heart weights.

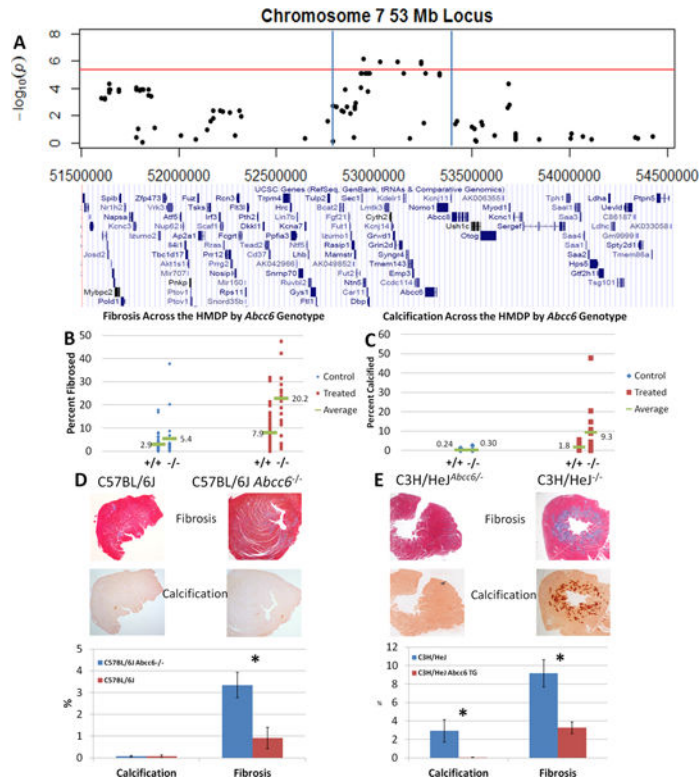


Figure 4. *Abcc6* plays a role in the regulation of cardiac fibrosis after ISO stimulation. **A)** The locus on chromosome 7 which contains *Abcc6* spans ~800kb and contains 28 genes within LD. **B)** Calcification in post-ISO treated hearts is increased in mice lacking *Abcc6*. **C)** Expression of *Abcc6* in a mouse that lacks the gene is sufficient to rescue the mouse from the ISO-induced fibrosis and calcification. **D)** Knockout of *Abcc6* in a mouse is sufficient to cause ISO-induced fibrosis, but does not cause a significant increase in calcification. WT n=4, KO n=3. **E)** The expression of *Abcc6* as a transgene is sufficient to significantly reduce both calcification and fibrosis. TG n=8, KO n=6. (*=P<0.05)

Table 1

Significant heart failure trait loci identified in HMDP GWA. The significance threshold is defined as p -value $< 4.1E-07$. RV, Liver, and Lung represents isoproterenol-treated right ventricular, liver and lung weights at week 3, respectively. Fibrosis represents isoproterenol-treated LV fibrosis at week 3. For each locus, the peak SNP location, given by chromosome (Chr) and base pair position (Bp) in the NCBI-build-37 assembly, and association p -value are reported, along with the number of genes (N) within the estimated LD block (LD) surrounding the peak SNP and the top candidate gene (Gene). Bold entries represent genes which contain nonsynonymous mutations within the HMDP as reported by the Wellcome Trust Mouse Genome Project, while underlined entries possess significant cis-eQTLs.

Phenotype	Chr	Bp	P-value	LD	N	Gene
Hypertrophic Loci						
RV	5	137934905	3.49E-10	137.93–138.15	11	<u>Mospd3</u>
RV	9	40202022	8.41E-08	39.77–40.52	15	<u>Scn3b</u>
RV	10	49818583	2.80E-07	48.19–54.24	22	<u>Pln</u>
RV Ratio	9	80542295	2.94E-07	80.00–80.99	2	<u>Myo6</u>
Fluid Retention Loci						
Liver	7	15251391	1.93E-07	15.13–18.75	57	<u>Calm3</u>
Lung	6	53975816	2.90E-07	53.88–55.57	17	<u>Aqp1</u>
Isoproterenol Treated Fibrosis Loci						
Fibrosis	X	10277028	4.10E-07	5–12.5	127	<u>Srpx</u>

Table 2

Suggestive heart failure trait loci identified in HMDP GWA. The suggestive threshold is defined as p-value < 4.1E-06. RV, Liver, and Lung represents isoproterenol-treated right ventricular, liver and lung weights at week 3, respectively. RV and RA ratio represents the ratio of isoproterenol-treated versus control Right Ventricle or Right Atrium weight at week 3. Fibrosis represents either control or isoproterenol-treated LV fibrosis at week 3. For each locus, the peak SNP location, given by chromosome (Chr) and base pair position (Bp) in the NCBI-build-37 assembly, and association p-value are reported, along with the number of genes (N) within the estimated LD block (LD) surrounding the peak SNP and the top candidate gene (Gene). Bold entries represent genes which contain nonsynonymous mutations within the HMDP as reported by the Wellcome Trust Mouse Genome Project, while underlined entries possess significant cis-eQTLs.

Phenotype	Chr	Bp	P-value	LD	N	Gene
Hypertrophic Loci						
RV	1	134467906	5.75E-07	133.78–134.53	14	–
RV	5	23873494	1.23E-06	23.82–24.47	20	<u><i>Prkag2</i></u>
RV	11	47181489	2.15E-06	46.18–49.3	41	<u><i>Sgcd</i></u>
RV Ratio	3	136305887	7.83E-07	136.04–136.79	1	<u><i>Ppp3ca</i></u>
RA Ratio	7	142011844	1.41E-06	141.50–144.81	15	<u><i>Mgmt</i></u>
Fluid Retention Loci						
Liver	10	49468021	3.48E-06	48.19–54.24	22	<u><i>Pln</i></u>
Lung	5	111867706	1.28E-06	110.87–112.87	22	<u><i>Miat</i></u>
Lung	7	81841621	3.88E-06	79.8–82.2	6	<u><i>Sltco3al</i></u> <u><i>Igsap1</i></u>
Lung	14	14941056	3.34E-06	8.5–21.5	50	<u><i>Ppp3cb</i></u>
Lung	19	27061190	2.01E-06	26.68–27.43	1	<u><i>Vldlr</i></u>
Baseline Fibrosis Loci						
Fibrosis	2	139163425	2.51E-06	13.7–14.0	6	<u><i>Jag1</i></u>
Fibrosis	4	84420058	2.20E-06	84–85	2	<u><i>Cntn1</i></u>
Fibrosis	7	73365047	1.31E-06	72.3–74.3	7	<u><i>Tjp1</i></u>
Isoproterenol Treated Fibrosis Loci						
Fibrosis	7	52946331	7.11E-07	52.85–53.42	28	<u><i>Abcc6</i></u>
Fibrosis	7	68593223	1.40E-06	60.5–69.5	18	<u><i>Surpn</i></u>
Fibrosis	7	73365047	1.40E-06	72.3–74.3	7	<u><i>Tjp1</i></u>

Phenotype	Chr	Bp	P-value	LD	N	Gene
Fibrosis	15	69907056	9.60E-07	68.4–71.4	3	<i>Col22a1</i>